Association of Macular and Circumpapillary Microvasculature with Visual Field Sensitivity in Advanced Glaucoma

ELHAM GHAHARI, CHRISTOPHER BOWD, LINDA M. ZANGWILL, JAMES PROUDFOOT, KYLE A. HASENSTAB, HUIYUAN HOU, RAFAELLA C. PENTEADO, PATRICIA ISABEL C. MANALASTAS, SASAN MOGHIMI, TAKUHEI SHOJI, MARK CHRISTOPHER, ADELEH YARMOHAMMADI, AND ROBERT N. WEINREB

• PURPOSE: To evaluate the association between optical coherence tomography angiography (OCTA) macular and circumpapillary vessel density and visual field mean deviation (MD) in advanced primary open angle glaucoma.

• DESIGN: Cross-sectional study.

• METHODS: Macula (superficial layer) and optic nerve head (ONH) with capillary density (CD) and without vessel density (VD) automated removal of large vessels OCTA of 34 eyes (34 patients, MD < -10 dB) were investigated as macula whole image VD (wiVD), parafoveal VD (pfVD), ONH wiVD, wiCD, circumpapillary VD, and cpCD. Spectral domain OCT circumpapillary retinal nerve fiber layer, macular ganglion cell complex, and ganglion cell inner plexiform layer were also analyzed.

• RESULTS: Macular and ONH VD decreased significantly with worsening MD. Each 1-dB decrease in MD was associated with a reduction of 0.43% and 0.46% for macular wiVD and pfVD with R^2 of 0.28 and 0.27, respectively (all $P < .01$). The association between MD and VD was strongest for measures of ONH with large vessels removed, wiCD, and cpCD, followed by wiVD and circumpapillary VD with R^2 of 0.26, 0.22, 0.17, 0.14, and a VD reduction of 0.43%, 0.51%, 0.33%, and 0.40%, respectively (all $P < .02$). There was a reduction of 1.19 μm in Avanti parafoveal ganglion cell complex, 1.13 μm in Spectralis ganglion cell inner plexiform layer, and 1.01 μm in Spectralis circumpapillary retinal nerve fiber layer, with R^2 of 0.19 ($P = .006$), 0.23 ($P = .002$), and 0.24 ($P = .002$), respectively.

• CONCLUSIONS: ONH and macula OCTA VD and thickness are associated with the severity of visual field damage in advanced primary open angle glaucoma. (Am J Ophthalmol 2019;204:51–61. © 2019 Elsevier Inc. All rights reserved.)

THE PATHOGENESIS OF PRIMARY OPEN ANGLE GLAUcoma (POAG) is not fully understood, but there is considerable evidence that vascular factors are involved.[1–3] Numerous methods have been used to evaluate the blood flow of the optic nerve and retina in order to gain insight into this relationship.[4–10] However, until recently there have not been robust methods available for studying the microvasculature and distinguishing the contributions of various vascular beds to optic nerve head (ONH) and retina perfusion in individuals with glaucoma. Optical coherence tomography angiography (OCTA) now provides qualitative and quantitative information of the perfused microvasculature of various retinal regions, including the optic nerve, peripapillary retina, and macula.[11–19]

Using a prototype OCTA system, Jia and associates[11] found that there was decreased optic disc perfusion in early to moderate glaucoma eyes compared with healthy eyes. It subsequently was reported that circumpapillary vessel density (VD) was reduced in glaucomatous eyes[13,20–22] and was highly correlated with visual field (VF) mean deviation (MD)[13,21] and OCT-measured tissue thickness.[23,24] Although it currently is well accepted that VF measurements are associated with vessel density and retinal nerve fiber layer (RNFL) tissue thickness in mild to moderate glaucoma, it has not been determined whether these relationships are maintained in advanced disease for OCTA VD and OCT tissue thickness measurements.

The purpose of the current study was to investigate whether macula and circumpapillary OCTA VD measurements have sufficient dynamic range to potentially detect disease-related change in advanced POAG by cross-sectionally assessing the associations between VF sensitivity and VD. Advanced glaucoma patients are of interest because the standard structural and functional tests used to detect progression are of diminished value.[25–29] Significant associations would suggest the possibility of detecting changes in VD for clinical management of advanced

Accepted for publication Mar 6, 2019.

From the Department of Ophthalmology, Hamilton Glaucoma Center, Shiley Eye Institute, and Viterbi Family Department of Ophthalmology, University of California San Diego, La Jolla, California, USA (E.G., C.B., L.M.Z., JP., K.A.H., H.H., R.C.P., P.I.C.M., S.M., T.S., M.C., A.Y., R.N.W.), and the Department of Ophthalmology, Saitama Medical University, Iruma, Saitama, Japan (T.S.).

Inquiries to Robert N. Weinreb, Hamilton Glaucoma Center, Shiley Eye Institute, and Viterbi Family Department of Ophthalmology, University of California San Diego, 9500 Gilman Drive 0946, La Jolla, CA 92093-0946, USA; e-mail: rweinreb@ucsd.edu

0002-9394/$36.00
https://doi.org/10.1016/j.ajo.2019.03.004

POAG and that this may inform glaucoma monitoring of such patients.

METHODS

THIS CROSS-SECTIONAL STUDY INCLUDED PATIENTS WITH advanced POAG who were enrolled in the Diagnostic Innovations in Glaucoma Study. The Diagnostic Innovations in Glaucoma Study is an ongoing prospective, longitudinal study at the Hamilton Glaucoma Center, University of California, San Diego (UCSD) that is designed to evaluate ocular anatomical structure and visual function in glaucoma. Details of the Diagnostic Innovations in Glaucoma Study protocol have been described previously.[30] All methods adhered to the tenets of the Declaration of Helsinki and the Health Insurance Portability and Accountability Act and were approved by the institutional review board at the UCSD. Informed consent was obtained from all participants.

One eye each from 34 POAG patients >18 years of age with best-corrected visual acuity ≥20/40, refractive error within ±5 diopters (D) sphere ±3 D cylinder and Humphrey VF MD worse than -10 dB were included. Patients with a history of ocular intervention other than uncomplicated cataract or uncomplicated glaucoma surgery, intraocular disease (e.g., diabetic retinopathy or nonglaucomatous optic neuropathy) or a systemic disease that could have had an impact on the study results (e.g., stroke or pituitary tumor) were excluded. Systemic hypertension and eyes with diabetes mellitus without retinopathy were not excluded.

POAG was defined as the presence of glaucomatous optic nerve damage (focal or diffuse neuroretinal rim narrowing and focal or diffuse atrophy of the circumpapillary RNFL) observed by masked stereoscopic optic disc photograph assessment with associated repeatable VF damage.

Standard automated perimetry was performed using the 24-2 Swedish Interactive Thresholding Algorithm protocol (HFA II 750i; Carl Zeiss Meditec Inc., Dublin, CA, USA). All participants were familiar with VF testing from previous exposure to ≥2 VF examinations. Glaucomatous VF damage was defined as a Glaucoma Hemifield Test outside of normal limits or a pattern standard deviation outside 95% normal limits confirmed on ≥2 consecutive tests and reviewed to have characteristic glaucomatous damage with similar patterns of VF damage across tests. VFs were reliable (fixation losses ≤33% and false positives ≤15%) with no evidence of rim or eyelid artifacts, inattention, or fatigue as assessed by UCSD Visual Field Assessment Center personnel.

All study participants underwent an ophthalmologic examination before study enrollment that included assessment of best-corrected visual acuity, slit-lamp biomicroscopy, intraocular pressure measurement with Goldmann applanation tonometry, gonioscopy, central corneal thickness measured with ultrasound pachymetry (DGH Technology Inc., Exton, PA, USA), dilated fundus examination, simultaneous stereophotography of the optic disc, and standard automated perimetry.

Systemic measurements included systolic and diastolic blood pressure and pulse rate measured with an automatic blood pressure instrument (model BP791IT; Omron Healthcare, Inc., Lake Forest, IL, USA). Mean arterial pressure was calculated as one third systolic blood pressure plus two-thirds diastolic blood pressure. Mean ocular perfusion pressure was defined as the difference between two-thirds of mean arterial pressure and intraocular pressure.

• **OPTICAL COHERENCE TOMOGRAPHY ANGIOGRAPHY AND SPECTRAL DOMAIN OCT:** OCTA and spectral domain OCT (SDOCT) imaging of the macula and optic nerve head (ONH) were performed with the Avanti SDOCT (version 2017.1.0.144; Optovue, Inc., Fremont, CA, USA). Using this system, OCTA and SDOCT measurements are obtained from the same scans allowing precise registration of the analyzed regions. OCTA and SDOCT parameters investigated are described below.

The Avanti AngioVue OCTA system uses split-spectrum amplitude-decorrelation angiography to capture the dynamic motion of red blood cells from sequential cross-sectional B-scans, providing high-resolution 3-dimensional visualization of vascular structures at various user-defined layers of the retina at the capillary level. Angiovue software automatically calculates VD as the percentage of measured area occupied by flowing blood vessels defined as pixels having decorrelation values above a set threshold level.

OCTA parameters investigated were macular whole image VD (wiVD), parafoveal macular VD (pfVD), whole image optic nerve head (ONH) VD without automated removal of large vessels (wiVD), whole image ONH VD with automated removal of large vessels (called whole image capillary densities [wiCD]), circumpapillary VD without automated removal of large vessels (cpVD), and circumpapillary VD with automated removal of large vessels (called circumpapillary capillary densities [cpCD]) (Figure 1). To generate a large vessel mask for the OCTA optic disc images, AngioVue software extracts vessels from the two-dimensional radial peripapillary capillary slab OCT en face image to construct a binary mask composed of vessels and nonvessels. Vessels of caliber ≥3 pixels are identified and excluded from analysis.

Macular whole image vessel density measurements were calculated from images acquired using the instrument-defined 3 × 3 mm^2 field of view (composed of merged Fast-X [horizontal] and Fast-Y [vertical] volume scans of 304 B-scans × 304 A-scans per B-scan) centered on the fovea within a slab defined as the volume from 3 μm below the internal limiting membrane to 15 μm below the inner

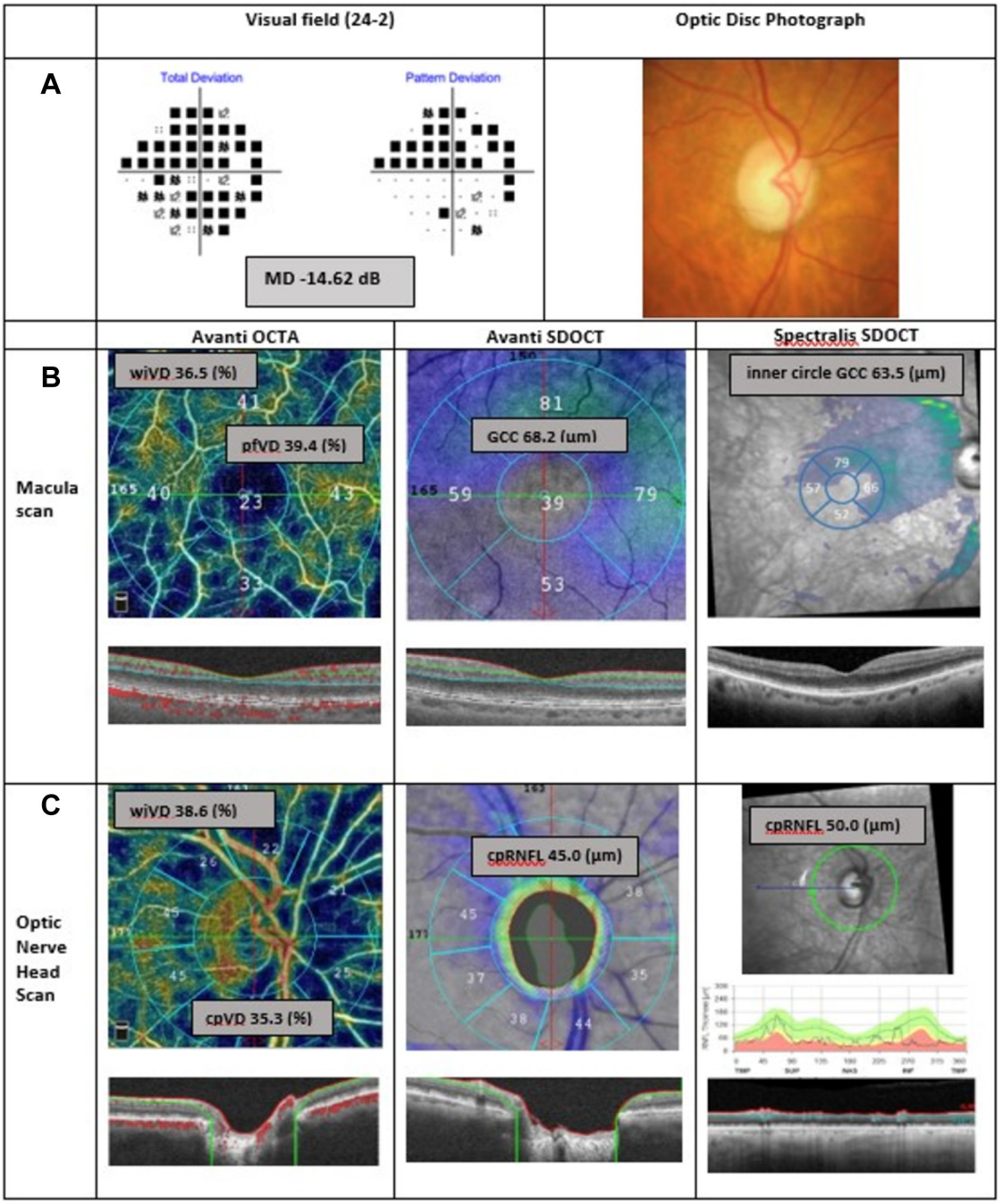

FIGURE 1. Representative eye with advanced glaucoma. (A) Visual field total and pattern deviation probability plots and optic disc photograph. (B) In the macula scan row, the first column shows Avanti optical coherence tomography angiography (OCTA), a vessel density map of the macular superficial layer showing reduced vessel density. The second column shows Avanti spectral domain OCT (SDOCT) and is an Avanti macular ganglion cell complex (GCC) thickness map. The final column shows Spectralis SDOCT, a Spectralis macular GCC layer thickness map. (C) In the optic nerve head scan row, Avanti OCTA shows a vessel density map of the peripapillary retinal nerve fiber layer (RNFL) illustrating reduced vessel density. In the second column, Avanti SDOCT shows a circumpapillary RNFL (cpRNFL) thickness map. In the final column, Spectralis SDOCT shows a Spectralis cpRNFL thickness map. cpCD = circumpapillary capillary density; cpVD = circumpapillary vessel density; MD = visual field mean deviation; pfVD = parafoveal vessel density; wiCD = whole image capillary density (vessel density after removing large vessel); wiVD = whole image vessel density.

plexiform layer (IPL). Parafoveal VD measurements were calculated from an instrument-defined annular region with an inner diameter of 1 mm and an outer diameter of 2.5 mm centered on the fovea.

Whole image ONH VD measurements were calculated from images acquired using the instrument-defined 4.5×4.5 mm^2 field of view (composed of merged Fast-X [horizontal] and Fast-Y [vertical] volume scans of 304 B-scans $\times$ 304 A-scans per B-scan) centered on the optic disc within a slab defined as the volume from the ILM to the posterior border of the RNFL.

Circumpapillary VD measurements were calculated from an instrument-defined 750-μm wide elliptical annulus extending from the optic disc boundary.

Macular ganglion cell complex thicknesses measurements were obtained from the same 3×3 mm^2 scans as macular VD measurements centered on the fovea from the internal limiting membrane to the IPL consisting of the ganglion cell layer, IPL, and RNFL. Circumpapillary RNFL thicknesses were calculated from the same 4.5×4.5 mm^2 field of view scans as ONH vessel densities centered on the optic disc.

Trained personnel reviewed the quality of all Avanti OCTA and SDOCT scans using a standard protocol established by the Imaging Data Evaluation and Analysis (IDEA) Center at UCSD. Poor-quality scans were excluded from the analysis if one of the following criteria were met: (1) signal strength index of <4 (with 1 = minimum, 10 = maximum); (2) poor clarity images; (3) local weak signal caused by artifacts, such as floaters; (4) residual motion artifacts visible as irregular vessel patterns or disc boundary on the enface angiogram; and (5) segmentation failure.

OCTA and OCT scans were obtained from both dilated and undilated eyes, with 65% obtained on the same day (i.e., both OCTA and OCTA images were obtained dilated or both images were obtained undilated). Previous work from our group suggests that that pre- and postdilation vessel density measurements are interchangeable (Villatoro G, et al. IOVS 2018;59:ARVO E-Abstract 2857).

To evaluate the generalizability of thickness measurement results across two different SDOCT devices, Spectralis SDOCT (version 5.2.0.3; Heidelberg Engineering GmbH, Heidelberg, Germany) also was used to evaluate cpRNFL thickness and macular thickness measurements. Spectralis uses a confocal laser-scanning ophthalmoscope with a wavelength of 870 nm and an infrared reference image to obtain images of ocular microstructures at an acquisition rate of 40,000 A-scans per second.

Spectralis SDOCT macular scans were obtained using the horizontal posterior pole asymmetry scan protocol. This scan protocol is composed of 61 B-scans spaced 120 μm apart with an optical resolution of 3.9 μm axially and 5.7 μm laterally covering an area of $30^\circ \times 25^\circ$ (6×6 mm).

After automated segmentation of each retinal layer, the Spectralis mapping software generated automated measurements of thickness of each retinal layer from the central 1-, 3-, and 6-mm circles as defined by the Early Treatment Diabetic Retinopathy Study. For direct comparison between Spectralis and Avanti OCT instruments, we calculated Spectralis Early Treatment Diabetic Retinopathy Study inner circle GC-IPL and ganglion cell complex measurements in the ring between the 1- and 3-mm circles.

Ganglion cell-inner plexifiorm layer (GC-IPL) thickness was calculated by adding ganglion cell and inner plexiform layers thicknesses and GCC thickness was calculated by adding ganglion cell, inner plexiform, and RNFL thicknesses.

Spectralis cpRNFL thickness was measured using the high-resolution circle scan protocol composed of a single B-scan of 1536 A-scans centered on the optic disc.

Similar to Avanti scans, the overall quality of Spectralis scans was evaluated by UC San Diego Imaging Data Evaluation and Analysis Center personnel. Images with noncentered scans, inaccurate segmentation of the cpRNFL, or quality scores ≤15 were excluded from the analyses. Avanti, Spectralis, and VF testing were completed within 6 months for all patients.

• **STATISTICAL ANALYSES:** Clinical characteristics, OCTA-derived vessel densities, and OCT-derived tissue thicknesses were described as mean values with associated 95% confidence intervals. Linear models were used to investigate univariable associations between VF MD and vessel density and tissue thickness measurements, with multivariable models fit including age and scan quality indices.

We also investigated the associations between all optical imaging parameters and VF total deviation mean sensitivity (TD). All statistical analyses were performed with R software (version 3.5.1). The alpha level (type I error) was set at 0.05.

RESULTS

THIRTY-FOUR EYES OF 34 PATIENTS WITH ADVANCED GLAUcoma were included in this cross-sectional study. A total of 11 eyes from 11 patients tested within the required 6-month window were excluded because of unacceptable image quality of ≥1 of the required images. Four eyes had both poor quality macula and ONH OCTA images, 4 eyes had poor quality ONH OCTA images (one of which also had a poor quality Spectralis RNFL image), and 3 eyes had poor quality macula OCTA images. Demographics and clinical characteristics of the study population are summarized in Table 1. Patients had a mean (95% confidence interval [CI]) age of 70.0 years (95% CI 65.9-72.1) years and

TABLE 1. Demographic and Ocular Characteristics

	Advanced Glaucoma in 34 Patients (n = 34 eyes)
Age (y)	70.0 (65.9-72.1)
Gender (%), male/female	22 (64.7)/12 (35.3)
Race, n (%)	Caucasian, 21 (61.8%); Black or African American, 6 (17.6%); Asian, 6 (17.6%); American Indian or Alaska Native, 1 (2.9%)
SBP (mm Hg)	125.4 (118.6-132.2)
DBP (mm Hg)	78.4 (74.1-82.6)
MOPP (mm Hg)	50.1 (46.9-53.2)
Self-reported diabetes, n (%)	4 (11.8)
Self-reported hypertension, n (%)	17 (50.0)
Visual field MD (dB)	-15.9 (-18.2 to -13.7)
Visual field TD (dB)	-8.1 (-9.8 to -6.4)
Visual field PSD (dB)	11.2 (10.4-11.9)
IOP (mm Hg)[a]	13.2 (11.5-14.9)
Axial length (mm)[b]	24.7 (24.0-25.4)
CCT (μm)[c]	522.6 (500.8-544.4)

Continuous variables are shown as mean (95% confidence interval).

CCT = central corneal thickness; dB = decibel; DBP = diastolic blood pressure; IOP = intraocular pressure; MD = mean deviation; MOPP = mean ocular perfusion pressure; PSD = pattern standard deviation; SBP = systolic blood pressure; TD = total deviation.

[a]Available for n = 32 eyes.

[b]Available for n = 30 eyes.

[c]Available for n = 22 eyes.

TABLE 2. Circumpapillary and Macular Structural and Vascular Measurements from Advanced Primary Open Angle Glaucoma Eyes

	Variables	Mean (95% CI)
Macula	Avanti wiVD (%)	38.2 (36.5-40.0)
	Avanti pfVD (%)	40.5 (38.5-42.5)
	Avanti parafovea GCC (μm)	79.5 (73.7-85.3)
	Spectralis GC-IPL (inner) (μm)	61.7 (56.7-66.6)
	Spectralis GCC (inner) (μm)	81.4 (75.5-87.3)
Optic nerve head	Avanti wiVD (%)	40.4 (38.7-42.0)
	Avanti wiCD (%)	34.1 (32.4-36.0)
	Avanti cpVD (%)	39.3 (37.2-41.5)
	Avanti cpCD (%)	33.1 (31.0-35.4)
	Avanti cpRNFL (μm)	56.8 (52.8-60.6)
	Spectralis cpRNFL (μm)	54.7 (50.4-59.0)

cpCD = circumpapillary capillary density; cpRNFL = circumpapillary retinal nerve fiber layer; cpVD = circumpapillary vessel density; GCC = ganglion cell complex; GC-IPL = ganglion cell inner plexiform layer; pfVD = parafoveal vessel density; wiCD = whole image capillary density (vessel density after removing large vessel); wiVD = whole image vessel density.

eyes had a mean (95% CI) MD of -15.9 dB (95% CI -18.2 to -13.7 dB).

OCTA-derived ONH, macular vessel densities, and SDOCT thickness measurements in the study population are shown in Table 2. The mean (95% CI) ONH vessel density measurements (Avanti wiVD 40.9% [95% CI 39.2-42.6] and cpVD 40.0% [95% CI 37.8-42.2]) without large vessel removal were larger than the ONH VD measurements with large vessel removal (Avanti wiCD 34.7% [95% CI 32.9-36.5] and cpCD 33.8% (95% CI 31.5-36.2). The Avanti and Spectralis GCC and cpRNFL thickness measures were similar.

The results of univariable and multivariable (adjusted for age and scan quality) linear regressions between vascular and structural parameters and visual field MD are shown in Table 3. Structure–function relationships with corresponding linear regression fits are shown in Figures 2 and 3.

Macular VD decreased with worsening VF MD with R^2 values of 0.28 ($P < .001$) and 0.27 ($P = .001$) for macular wiVD and pfVD, respectively. Each 1-dB decrease in VF MD was associated with a reduction of 0.43% in macular wiVD and 0.46% in pfVD.

The association between ONH VD and VF MD was strongest after removal of large vessels. R^2 values for ONH wiCD, cpCD, wiVD, and cpVD were 0.26, 0.22, 0.17, and 0.14 respectively (all $P < .02$) (Table 3). Each 1-dB decrease in VF MD was associated with a 0.51% reduction in cpCD, a 0.43% reduction in wiCD, a 0.40% reduction in cpVD, and a 0.33% reduction in wiVD.

Macular thickness measurements also were significantly associated with VF MD (R^2 was 0.19 for Avanti pfGCC, 0.21 for Spectralis inner circle GCC, and 0.23 for Spectralis inner circle GC-IPL, all $P < .05$). Each 1-dB decrease in VF MD was associated with a 1.19-μm reduction in Avanti pfGCC thickness, a 1.28-μm reduction in Spectralis GCC (inner circle) thickness, and a 1.13-μm reduction in Spectralis GC-IPL (inner circle) thickness (all $P < .01$).

Although Spectralis SDOCT cpRNFL thickness measurements were significantly associated with VF MD (R^2 0.24, $P = .002$), Avanti cpRNFL thickness measurements were not (R^2 0.02, $P = .209$). Each 1-dB decrease in VF MD was associated with a 1.01-μm reduction in Spectralis-measured cpRNFL thickness.

In multivariable analyses, the regression coefficient (β) between VF MD and all macular and ONH VD measurements, parafoveal GCC thickness, and Spectralis-measured cpRNFL measurements remained significant after controlling for scan quality and age as potential confounding factors (all $P \leq .05$).

The results of univariable and multivariable (adjusted for age and scan quality index) linear regressions

TABLE 3. Linear Regression Results Describing the Relationships Between VF MD and Macular and ONH Measures

		Univariable			Multivariable		
	Variable	β (95% CI)	*P* Value	R^2	β (95% CI)	*P* Value	R^2
Macula	Avanti wiVD (%)	0.43 (0.19-0.66)	<.001	0.28	0.49 (0.27-0.71)	<.001	0.40
	Avanti pfVD (%)	0.46 (0.20-0.72)	.001	0.27	0.52 (0.27-0.77)	<.001	0.39
	Avanti Parafovea GCC (μm)	1.19 (0.36-2.01)	.006	0.19	1.26 (0.41-2.12)	.005	0.18
	Spectralis GC-IPL (Inner) (μm)	1.13 (0.43-1.82)	.002	0.23	1.26 (0.44-2.07)	.004	0.20
	Spectralis GCC (Inner) (μm)	1.28 (0.45-2.11)	.004	0.21	1.48 (0.50-2.45)	.004	0.18
ONH	Avanti wiVD (%)	0.33 (0.09-0.57)	.009	0.17	0.37 (0.13-0.62)	.004	0.19
	Avanti wiCD (%)	0.43 (0.18-0.67)	.001	0.26	0.47 (0.22-0.71)	<.001	0.31
	Avanti cpVD (%)	0.40 (0.08-0.71)	.016	0.14	0.46 (0.14-0.78)	.007	0.18
	Avanti cpCD (%)	0.51 (0.18-0.83)	.003	0.22	0.57 (0.24-0.89)	.001	0.26
	Avanti cpRNFL (μm)	0.39 (-0.23 to 1.02)	.209	0.02	0.39 (-0.26 to 1.04)	.229	−0.01
	Spectralis cpRNFL (μm)	1.01 (0.41-1.61)	.002	0.24	0.89 (0.26-1.51)	.007	0.25

Multivariable models are adjusted for age and scan quality index.

CI = confidence interval; cpCD = circumpapillary capillary density; cpRNFL = circumpapillary retinal nerve fiber layer; cpVD = circumpapillary vessel density; GCC = ganglion cell complex; GC-IPL = ganglion cell inner plexiform layer; ONH = optic nerve head; pfVD = parafoveal vessel density; VF MD = visual field mean deviation; wiCD = whole image capillary density (vessel density after removing large vessel); wiVD = whole image vessel density.

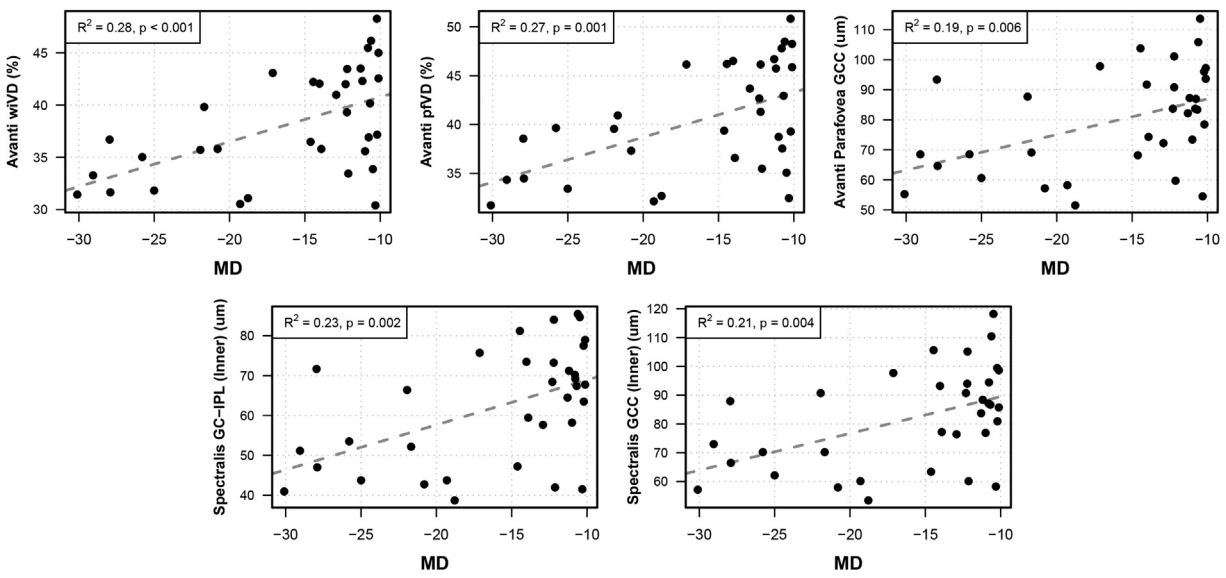

FIGURE 2. Scatter plots showing the best fit linear regression line between visual field mean deviation (MD) and macular optical coherence tomography angiography whole image vessel density (Avanti wiVD), parafoveal vessel density (Avanti pfVD), parafoveal ganglion cell complex (Avanti parafoveal GCC), and ganglion cell inner plexiform layer (Spectralis GC-IPL).

between vascular and structural parameters and VF TD mean sensitivity expressed in dB are shown in Table 4. The relative magnitude of R^2 values among associations of OCTA and SDOCT measurements using VF TD mean sensitivity were similar to the relative magnitude of R^2 values among associations between OCTA and SDOCT measurements and VF MD.

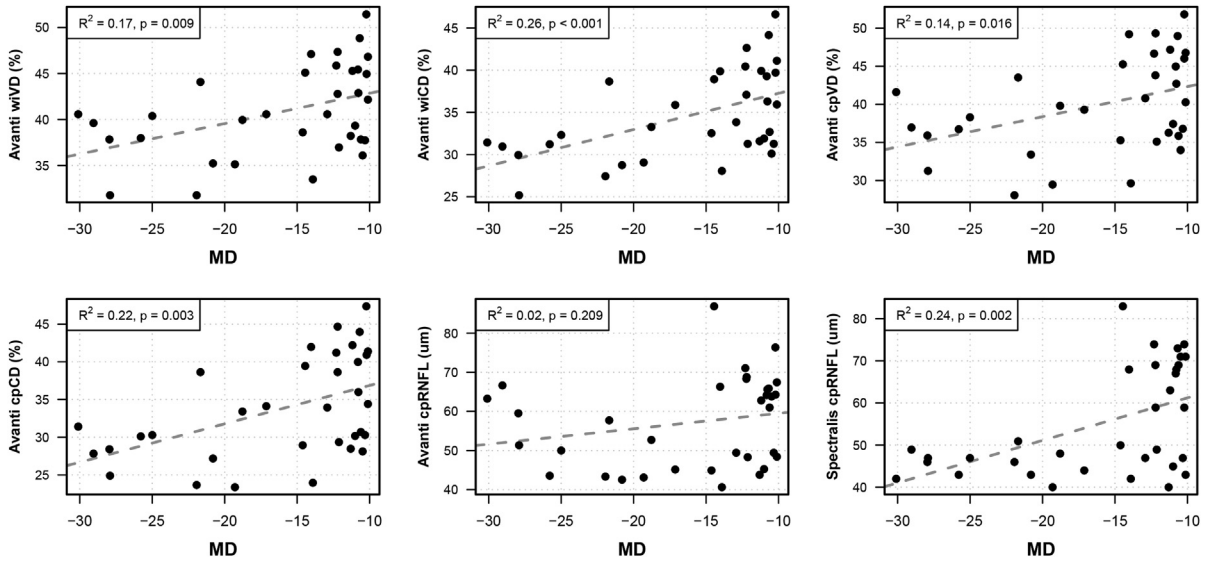

FIGURE 3. Scatter plots showing the best fit linear regression line between visual field mean deviation and peripapillary optic nerve head optical coherence tomography angiography and thickness measurements. cpCD = circumpapillary capillary density; cpRNFL = circumpapillary retinal nerve fiber layer; cpVD = circumpapillary vessel density; MD = visual field mean deviation; wiCD = whole image capillary density (vessel density after removing large vessel); wiVD = whole image vessel density.

DISCUSSION

IN THE CURRENT STUDY, MACULA AND CIRCUMPAPILLARY VDs were significantly associated with severity of visual field loss measured as MD and TD mean sensitivity in advanced POAG eyes. Macular thickness measurements (GCC and GC-IPL) and Spectralis cpRNFL thickness also were associated with severity of loss in our sample. These cross-sectional results have important implications for monitoring patients with advanced glaucoma in whom detection of progression is particularly difficult as the standard structural and functional tests used are of reduced value.[25–29] Specifically, these results suggest that vascular and structural measures of the ONH and macula may be useful parameters for monitoring progression in advanced glaucoma, particularly if confirmed by longitudinal studies.

OCTA studies have shown decreased circumpapillary VD in glaucoma eyes with increasing severity of disease, suggesting possible use of VD measurements for detecting glaucomatous progression, but there is limited information on vascular dropout in advanced disease.[12,20,21,31,32] With recent evidence demonstrating the importance of evaluating macula damage in glaucoma in early, moderate, and particularly advanced disease,[26,27,33,34] we chose to investigate both OCTA macular and peripapillary VDs and compare their association with VF severity to that of SDOCT thickness measurements in advanced glaucoma to determine if these measurements could be useful for monitoring change in severe disease.

The current results are consistent with previous studies that reported that decreased cpVD was significantly associated with the severity of VF damage along the glaucoma severity continuum.[21,35,36] As expected, we also found that the association between ONH vasculature and MD was strongest after removing larger vessels from image analysis. This is explained by the fact that larger vessels contribute to increased VD measurements but likely are not affected by glaucoma; therefore, they are not likely to contribute to the decrease in VD expected with the decrease in MD. Moreover, the impact of large vessels on VD measurements is higher in advanced disease because large vessels make up a larger proportion of vessel density in advanced disease compared with early and moderate glaucoma.[37]

Although the strength of the association between VF severity and macular VD was similar to that of circumpapillary VD and macular and RNFL thickness measures in univariable analysis, in multivariable analysis after adjusting for age and scan quality index, the association between visual field MD and macula whole image vessel density ($R^2 = .40$) was stronger than ONH whole image capillary density ($R^2 = 0.31$) and GCC and RNFL thicknesses. The multivariable results suggesting a stronger relationship between macula VD measures compared with ONH VD measures with the severity of VF damage in advanced glaucoma are consistent with previous studies that found ganglion cell inner plexiform layer thickness has a stronger relationship with VF severity than RNFL thickness in advanced disease.[27,29] The stronger association between VF MD and both macular wiVD and pfVD in

TABLE 4. Linear Regression Results Describing the Relationships Between VF TD (dB) and Macular and ONH Measures

		Univariable			Multivariable		
	Variable	β (95% CI)	*P* Value	R^2	β (95% CI)	*P* Value	R^2
Macula	Avanti wiVD (%)	0.57 (0.27-0.88)	<.001	0.29	0.65 (0.36-0.94)	<.001	0.41
	Avanti pfVD (%)	0.63 (0.29-0.97)	<.001	0.29	0.71 (0.39-1.03)	<.001	0.41
	Avanti Parafovea GCC (μm)	1.73 (0.68-2.79)	.002	0.24	1.86 (0.77-2.95)	.002	0.24
	Spectralis GC-IPL (Inner) (μm)	1.60 (0.71-2.49)	<.001	0.27	1.75 (0.73-2.77)	.001	0.25
	Spectralis GCC (Inner) (μm)	1.82 (0.76-2.89)	.001	0.25	2.04 (0.81-3.27)	.002	0.22
ONH	Avanti wiVD (%)	0.45 (0.13-0.77)	.007	0.18	0.53 (0.21-0.85)	.002	0.23
	Avanti wiCD (%)	0.59 (0.28-0.91)	<.001	0.29	0.68 (0.37-0.99)	<.001	0.37
	Avanti cpVD (%)	0.52 (0.10-0.94)	.017	0.14	0.63 (0.20-1.06)	.005	0.19
	Avanti cpCD (%)	0.69 (0.27-1.11)	.002	0.23	0.81 (0.38-1.23)	<.001	0.30
	Avanti cpRNFL (μm)	0.56 (-0.26 to 1.38)	.173	0.03	0.62 (-0.25 to 1.48)	.154	0.01
	Spectralis cpRNFL (μm)	1.34 (0.54-2.13)	.002	0.25	1.20 (0.35-2.05)	.007	0.25

Multivariable models are adjusted for age and scan quality index.

CI = confidence interval; cpCD = circumpapillary capillary density; cpRNFL = circumpapillary retinal nerve fiber layer; cpVD = circumpapillary vessel density; dB = decibel; GCC = ganglion cell complex; GC-IPL = ganglion cell inner plexiform layer; ONH = optic nerve head; pfVD = parafoveal vessel density; VF TD = visual field total deviation; wiCD = whole image capillary density (vessel density after removing large vessel); wiVD = whole image vessel density.

multivariable analyses compared with univariable analyses is the stronger effect of age on the macula vessel measurements ($P < .05$); age was not significantly associated with the ONH VD or macula and ONH thickness measures ($P > .05$).

In the current study, we also found that both SDOCT macula and ONH parapapillary thickness measurements were both associated with the severity of VF loss in advanced glaucoma and that results are not necessarily generalizable across OCT instruments. Specifically, we found that both Avanti and Spectralis GCC thickness measurements showed a similar strength of association (R^2) with the severity of visual field loss measured by MD (R^2 values of 0.19 and 0.21, respectively), and TD mean sensitivity (dB) (R^2 values of 0.24 and 0.25, respectively). However, Spectralis-measured cpRNFL thickness, but not Avanti-measured cpRNFL thickness, was significantly associated with VF MD and TD mean sensitivity. There are several possible explanations for the differences between these associations. As previously reported,[38] RNFL thickness measurements vary across OCT instruments. In addition, Spectralis obtains images at higher resolution than Avanti (3.9 μm axially and 5.7 μm laterally vs. 5 μm axially and 15 μm laterally, respectively), there are different proprietary segmentation algorithms and slightly different scan locations. Moreover, there is evidence that the dynamic range of Spectralis RNFL thickness measurements is larger and the measurement floor lower compared with Avanti, which could affect strengths of associations in advanced disease.[39] The current study is unique in that it reports the associations of RNFL and macular thickness with severity of VF damage using 2 different OCT instruments. The current results for cpRNFL thickness further emphasize the importance of not generalizing results across SDOCT instruments and, although not tested in the current study, across different OCTA instruments.[40,41]

In contrast to the current study, other studies that included more severe glaucoma reported that GCC and GC-IPL measurements were more strongly associated with VF MD than cpRNFL. This is likely because of the reported measurement floor of approximately 50 μm in Spectralis-measured RNFL thickness in eyes with VF defects worse than approximately -15 dB MD.[26,28,42–44] It is possible that this floor was not observed in the current study because some eyes with less advanced glaucoma were included. Further inspection of Figure 3 (bottom row, far right panel) suggests that the slope of a linear fit for MD between approximately -15 dB and -30 dB would be a flat line. That is, the observed significant association was driven primarily by a concentration of eyes with MD closer to -10 dB.

We recently reported longitudinal results that GC-IPL and a novel 3-dimensional whole volume measurement based on Bayesian kernel detection can detect significant change in advanced POAG eyes with VF MD between -12 dB and -22 dB.[26,27] In addition, GC-IPL thickness was less likely than cpRNFL thickness and Bruch membrane opening minimum rim width to reach a measurement floor in advanced glaucoma eyes. The current study results are consistent with previous results and suggest that GC-IPL thickness is an informative parameter for detecting disease-related changes in advanced glaucoma because of the relatively larger dynamic range of GC-IPL thickness compared with GCC and cpRNFL.[27,28]

Several studies have suggested that OCTA vessel density measurements have similar diagnostic classification ability compared with OCT tissue thickness measurements.[24,45,46] In addition, baseline OCTA parameters are reportedly associated with a faster rate of RNFL progression in mild to moderate glaucoma, suggesting that decreased VD may be a risk indicator for progression.[47] Our multivariable results suggest that VD measures tend to be more strongly associated with severity of VF damage than thickness measures and may be an additional tool to monitor progression in advanced disease. This suggestion is particularly valuable for the detection of progression in advanced disease, although longitudinal studies are needed to confirm these cross-sectional findings. In addition, newly available measures of vascular factors, such as VD, likely will provide additional information regarding the pathogenesis of glaucoma in the long term. It also should be mentioned that possible disadvantages of OCTA measurements include a higher rate of inadequate quality scans and poorer reproducibility[48] compared with OCT thickness measures, although this may not be the case for all OCTA instruments because software analytics vary across imaging platforms.

There are several possible limitations to the present study. This study was cross-sectional and therefore we could not detect the temporal relationship between VF progression and loss of VD and tissue thickness. Longitudinal studies can further clarify these relationships. In addition, potentially confounding effects of intraocular pressure–lowering medications, blood pressure–lowering medications, and systemic conditions on VD measurements were not evaluated. The effect of these factors on vascular measurements cannot be dismissed. Finally, it is possible that the associations between structural and functional measurements varied in strength across the observed range of MD within the current cohort. To address this, we examined the absolute standardized residuals from each model against MD. We did not find any systematic evidence that residuals grew larger with more advanced disease. In addition, standardized residual plots versus fitted values did not indicate a significant departure from a linear relationship between MD and each outcome.

In conclusion, OCTA-measured circumpapillary and macular VDs, particularly circumpapillary VDs calculated after large vessel removal, as well as cpRNFL, GCC, and GC-PIL thickness, are associated with the severity of visual field damage in advanced POAG. Longitudinal studies are needed to determine the relative importance of these measures for detecting glaucomatous progression in advanced disease.

FUNDING/SUPPORT: THIS STUDY WAS SUPPORTED BY NATIONAL INSTITUTES OF HEALTH/NATIONAL EYE INSTITUTE GRANTS R01EY029058, R01EY011008, R01 EY14267, and R01 EY027510, Core Grant P30EY022589, an unrestricted grant from Research to Prevent Blindness (New York, NY USA), and grants for participants' glaucoma medications from Alcon, Allergan, Pfizer, Merck, and Santen. Financial Disclosures: Takuhei Shoji has received funding from Pfizer, Senju, Alcon, Santen, Kowa, and Otsuka. Linda M. Zangwill has received funding from the National Eye Institute, Carl Zeiss Meditec., Heidelberg Engineering GmbH, Optovue Inc., Topcon Medical Systems Inc., and Heidelberg Engineering. Robert N. Weinreb has received funding from Aerie Pharmaceuticals, Allergan, Eyenovia, Implantdata, Sensimed, Unity Biotechnology, Valeant, Heidelberg Engineering, Carl Zeiss Meditec, Genentech, Konan, Optovue, Topcon, Optos, Centervue, Bausch and Lomb, Toromedes, and Meditec-Zeiss. The following authors have no financial disclosures: Elham Ghahari, Huiyuan Hou, Sasan Moghimi, Patricia Isabel C. Manalastas, Rafaella C. Penteado, Adeleh Yarmohammadi, Mark Christopher, Kyle Hasenstab, Christopher Bowd, and James Proudfoot. All authors attest that they meet the current ICMJE criteria for authorship.

REFERENCES

1. Weinreb RN, Khaw PT. Primary open-angle glaucoma. *Lancet* 2004;363:1711–1720.
2. Leske MC, Wu SY, Hennis A, Honkanen R, Nemesure B, BESs Study Group. Risk factors for incident open-angle glaucoma: the Barbados Eye Studies. *Ophthalmology* 2008;115(1):85–93.
3. Leske MC, Heijl A, Hyman L, et al. Predictors of long-term progression in the Early Manifest Glaucoma Trial. *Ophthalmology* 2007;114(11):1965–1972.
4. O'Brart DP, de Souza Lima M, Bartsch DU, Freeman W, Weinreb RN. Indocyanine green angiography of the peripapillary region in glaucomatous eyes by confocal scanning laser ophthalmoscopy. *Am J Ophthalmol* 1997;123(5):657–666.
5. Rechtman E, Harris A, Kumar R, et al. An update on retinal circulation assessment technologies. *Curr Eye Res* 2003;27(6):329–343.
6. Plange N, Kaup M, Weber A, Remky A, Arend O. Fluorescein filling defects and quantitative morphologic analysis of the optic nerve head in glaucoma. *Arch Ophthalmol* 2004;122(2):195–201.
7. Nicolela MT, Hnik P, Drance SM. Scanning laser Doppler flowmeter study of retinal and optic disk blood flow in glaucomatous patients. *Am J Ophthalmol* 1996;122(6):775–783.
8. Michelson G, Schmauss B, Langhans MJ, Harazny J, Groh MJ. Principle, validity, and reliability of scanning laser Doppler flowmetry. *J Glaucoma* 1996;5(2):99–105.
9. Petrig BL, Riva CE, Hayreh SS. Laser Doppler flowmetry and optic nerve head blood flow. *Am J Ophthalmol* 1999;127(4):413–425.
10. Yaoeda K, Shirakashi M, Funaki S, Funaki H, Nakatsue T, Abe H. Measurement of microcirculation in the optic nerve head by laser speckle flowgraphy and scanning laser Doppler flowmetry. *Am J Ophthalmol* 2000;129(6):734–739.
11. Jia Y, Wei E, Wang X, et al. Optical coherence tomography angiography of optic disc perfusion in glaucoma. *Ophthalmology* 2014;121(7):1322–1332.
12. Yu J, Jiang C, Wang X, et al. Macular perfusion in healthy Chinese: an optical coherence tomography angiogram study. *Invest Ophthalmol Vis Sci* 2015;56(5):3212–3217.

13. Liu L, Jia Y, Takusagawa HL, et al. Optical coherence tomography angiography of the peripapillary retina in glaucoma. *JAMA Ophthalmol* 2015;133(9):1045–1052.
14. Zhang M, Hwang TS, Dongye C, Wilson DJ, Huang D, Jia Y. Automated quantification of nonperfusion in three retinal plexuses using projection-resolved optical coherence tomography angiography in diabetic retinopathy. *Invest Ophthalmol Vis Sci* 2016;57(13):5101–5106.
15. Matsunaga DR, Yi JJ, De Koo LO, Ameri H, Puliafito CA, Kashani AH. Optical coherence tomography angiography of diabetic retinopathy in human subjects. *Ophthalmic Surg Laser Imaging Retina* 2015;46(8):796–805.
16. Sulzbacher F, Pollreisz A, Kaider A, et al. Identification and clinical role of choroidal neovascularization characteristics based on optical coherence tomography angiography. *Acta Ophthalmol* 2017;95(4):414–420.
17. Shahlaee A, Samara WA, Hsu J, et al. In vivo assessment of macular vascular density in healthy human eyes using optical coherence tomography angiography. *Am J Ophthalmol* 2016; 165:39–46.
18. Lee J, Moon BG, Cho AR, Yoon YH. Optical coherence tomography angiography of DME and its association with Anti-VEGF treatment response. *Ophthalmology* 2016;123(11): 2368–2375.
19. Spaide RF, Klancnik JM Jr, Cooney MJ. Retinal vascular layers imaged by fluorescein angiography and optical coherence tomography angiography. *JAMA Ophthalmol* 2015; 133(1):45–50.
20. Bojikian KD, Chen CL, Wen JC, et al. Optic disc perfusion in primary open angle and normal tension glaucoma eyes using optical coherence tomography-based microangiography. *PLoS One* 2016;11(5):e0154691.
21. Yarmohammadi A, Zangwill LM, Diniz-Filho A, et al. Relationship between optical coherence tomography angiography vessel density and severity of visual field loss in glaucoma. *Ophthalmology* 2016;123(12):2498–2508.
22. Rao HL, Pradhan ZS, Weinreb RN, et al. Regional comparisons of optical coherence tomography angiography vessel density in primary open-angle glaucoma. *Am J Ophthalmol* 2016;171:75–83.
23. Mammo Z, Heisler M, Balaratnasingam C, et al. Quantitative optical coherence tomography angiography of radial peripapillary capillaries in glaucoma, glaucoma suspect, and normal eyes. *Am J Ophthalmol* 2016;170:41–49.
24. Chen CL, Zhang A, Bojikian KD, et al. Peripapillary retinal nerve fiber layer vascular microcirculation in glaucoma using optical coherence tomography-based microangiography. *Invest Ophthalmol Vis Sci* 2016;57(9):475–485.
25. Gardiner SK, Swanson WH, Goren D, Mansberger SL, Demirel S. Assessment of the reliability of standard automated perimetry in regions of glaucomatous damage. *Ophthalmology* 2014;121(7):1359–1369.
26. Bowd C, Zangwill LM, Weinreb RN, Medeiros FA, Belghith A. Estimating optical coherence tomography structural measurement floors to improve detection of progression in advanced glaucoma. *Am J Ophthalmol* 2017; 175:37–44.
27. Belghith A, Medeiros FA, Bowd C, et al. Structural change can be detected in advanced-glaucoma eyes. *Invest Ophthalmol Vis Sci* 2016;57(9):511–518.
28. Shin JW, Sung KR, Lee GC, Durbin MK, Cheng D. Ganglion cell-inner plexiform layer change detected by optical coherence tomography indicates progression in advanced glaucoma. *Ophthalmology* 2017;124(10):1466–1474.
29. Sung MS, Kang BW, Kim HG, Heo H, Park SW. Clinical validity of macular ganglion cell complex by spectral domain-optical coherence tomography in advanced glaucoma. *J Glaucoma* 2014;23(6):341–346.
30. Sample PA, Girkin CA, Zangwill LM, et al. The African Descent and Glaucoma Evaluation Study (ADAGES): design and baseline data. *Arch Ophthalmol* 2009;127(9): 1136–1145.
31. Rao HL, Pradhan ZS, Weinreb RN, et al. A comparison of the diagnostic ability of vessel density and structural measurements of optical coherence tomography in primary open angle glaucoma. *PLoS One* 2017;12(3):e0173930.
32. Akagi T, Iida Y, Nakanishi H, et al. Microvascular density in glaucomatous eyes with hemifield visual field defects: an optical coherence tomography angiography study. *Am J Ophthalmol* 2016;168:237–249.
33. Hood DC, Raza AS, deMoraes CG, Liebmann JM, Ritch R. Glaucomatous damage of the macula. *Prog Retin Eye Res* 2013;32:1–21.
34. Hood DC. Improving our understanding, and detection, of glaucomatous damage: An approach based upon optical coherence tomography (OCT). *Prog Retin Eye Res* 2017;57: 46–75.
35. Rao HL, Pradhan ZS, Weinreb RN, et al. Vessel density and structural measurements of optical coherence tomography in primary angle closure and primary angle closure glaucoma. *Am J Ophthalmol* 2017;177:106–115.
36. Rao HL, Pradhan ZS, Weinreb RN, et al. Relationship of optic nerve structure and function to peripapillary vessel density measurements of optical coherence tomography angiography in glaucoma. *J Glaucoma* 2017;26(6):548–554.
37. Yu PK, Cringle SJ, Yu DY. Correlation between the radial peripapillary capillaries and the retinal nerve fibrer layer in the normal human retina. *Exp Eye Res* 2014;129:83–92.
38. Leite MT, Rao HL, Weinreb RN, et al. Agreement among spectral-domain optical coherence tomography instruments for assessing retinal nerve fiber layer thickness. *Am J Ophthalmol* 2011;151(1):85–92.
39. Mwanza JC, Kim HY, Budenz DL, et al. Residual and dynamic range of retinal nerve fiber layer thickness in glaucoma: comparison of three OCT platforms. *Invest Ophthalmol Vis Sci* 2015;56(11):6344–6351.
40. Pilotto E, Frizziero L, Crepaldi A, et al. Repeatability and reproducibility of foveal avascular zone area measurement on normal eyes by different optical coherence tomography angiography instruments. *Ophthalmic Res* 2018;59:206–211.
41. Shiihara H, Sakamoto T, Yamashita T, et al. Reproducibility and differences in area of foveal avascular zone measured by three different optical coherence tomographic angiography instruments. *Sci Rep* 2017;7(1):9853.
42. Hood DC, Anderson SC, Wall M, Kardon RH. Structure versus function in glaucoma: an application of a linear model. *Invest Ophthalmol Vis Sci* 2007;48(4):3662–3668.
43. Hood DC, Kardon RH. A framework for comparing structural and functional measures of glaucomatous damage. *Prog Retin Eye Res* 2007;26(6):688–710.

44. Mwanza JC, Budenz DL, Warren JL, et al. Retinal nerve fibre layer thickness floor and corresponding functional loss in glaucoma. *Br J Ophthalmol* 2015;99(6):732–737.
45. Yarmohammadi A, Zangwill LM, Diniz-Filho A, et al. Optical coherence tomography angiography vessel density in healthy, glaucoma suspect, and glaucoma eyes. *Invest Ophthalmol Vis Sci* 2016;57(9):451–459.
46. Rao HL, Kadambi SV, Weinreb RN, et al. Diagnostic ability of peripapillary vessel density measurements of optical coherence tomography angiography in primary open-angle and angle-closure glaucoma. *Br J Ophthalmol* 2017;101:1066–1070.
47. Moghimi S, Zangwill LM, Penteado RC, et al. Macular and optic nerve head vessel density and progressive retinal nerve fiber layer loss in glaucoma. *Ophthalmology* 2018;125:1720–1728.
48. Manalastas PIC, Zangwill LM, Saunders LJ, et al. Reproducibility of optical coherence tomography angiography macular and optic nerve head vascular density in glaucoma and healthy eyes. *J Glaucoma* 2017;26(10):851–859.